

1 **Review assay**

2

3 **Sorting of cargo in the tubular endosomal network**

4

5 Jachen A. Solinger and Anne Spang\*

6

7 Biozentrum, University of Basel, Spitalstrasse 41, CH-4056 Basel, Switzerland

8

9 \*Corresponding Author:

10 Anne Spang, ORCID:0000-0002-2387-6203

11 Biozentrum

12 University of Basel

13 Spitalstrasse 41

14 CH-4056 Basel

15 Switzerland

16

17 Email: [anne.spang@unibas.ch](mailto:anne.spang@unibas.ch)

18 Phone: +41 61 207 2380

19

20 Keywords: tether, recycling endosomes, endocytosis, small GTPases, Sec1/Munc18  
21 protein, SNAREs, vesicle transport, Rab proteins, membrane fusion, membrane  
22 fission, adaptor proteins, tubular endosomal networks

23

24 Abbreviations:

25 FERARI: Factors for endosome recycling and Rab interactions

26 TEN: tubular endosomal networks

27 TGN: trans-Golgi network

28 SE: sorting endosome

29

30

31

32 **Abstract**

33

34 Intercellular communication is an essential process in all multicellular organisms.  
35 During this process, molecules secreted by one cell will bind to a receptor on the  
36 cognate cell leading to the subsequent uptake of the receptor-ligand complex. Once  
37 inside, the cell then determines the fate of the receptor-ligand complex and any other  
38 proteins that were endocytosed together. Approximately 80% of endocytosed  
39 material is recycled back to the plasma membrane either directly or indirectly via the  
40 Golgi apparatus and the remaining 20% is delivered to the lysosome for degradation.  
41 Although most pathways have been identified, we still lack understanding on how  
42 specificity in sorting of recycling cargos into different pathways is achieved, and how  
43 the cell reaches high accuracy of these processes in the absence of clear sorting  
44 signals in the bulk of the client proteins. In this review, we will summarize our current  
45 understanding of the mechanism behind recycling cargo sorting and propose a  
46 model of differential affinities between cargo and cargo receptors/adaptors with  
47 regards to iterative sorting in endosomes.

48

49

50 **Introduction**

51

52 The biosynthetic and the endocytic routes of the intracellular transport pathway  
53 converge on endosomes where cargos destined for the plasma membrane are  
54 delivered either by a direct route (biosynthetic route) or via a recycling pathway (after  
55 endocytosis). During this process both the newly synthesized and recycled cargo  
56 proteins frequently share the same transport container on their way to the plasma  
57 membrane. However, the plasma membranes of most cells are compartmentalized  
58 into functionally different domains often accompanied by characteristic structural  
59 features. This compartmentalization is easily appreciated in polarized epithelial cells  
60 in which the apical, lateral and basal plasma membrane compartments are clearly  
61 distinguishable. Furthermore, plasma membrane compartmentalization also exists at  
62 a much smaller scale including sites of nutrient uptake, cell-to-cell communication,  
63 as well as the plasma membrane contact sites with the endoplasmic reticulum and  
64 other organelles. Each of these compartments must be populated with a distinct  
65 profile of membrane proteins at the proper concentration and the maintenance of  
66 these compartments is dependent on the correct balance of exo- and endocytosis.  
67 Transport carriers destined for the plasma membrane may contain cargo for either  
68 specific domains or for multiple domains, which could then be sorted later into  
69 different compartments. Thus, different cargo exit sites should exist at the  
70 endosomes and the trans Golgi Network (TGN) comparable to taxis and public  
71 transport systems. In support of this concept, cells appear to employ both types of  
72 transport systems as there are specialized transport vesicles (Spang, 2015) as well  
73 as more generic carriers (i.e. clathrin-coated vesicles).

74

75 Although we have a good understanding of the different routes of endocytosis such  
76 as the clathrin-dependent endocytosis pathway (Mayor and Pagano, 2007; Mettlen  
77 et al., 2018; Weinberg and Drubin, 2012), the downstream events in endocytosis and  
78 regulation thereof, which includes sorting and recycling, are much less clear. One  
79 contributing factor is that the presence or absence of a molecule from the plasma  
80 membrane is more easily assessed by light microscopy and biochemical methods  
81 compared to a protein that moves within the cell. Another reason is the diverse  
82 morphological features of the endosomal system (Fig. 1), which consists of tubular  
83 endosomal networks (TEN) also referred to as tubular-vesicular clusters, round  
84 empty or filled looking structures, multivesicular bodies, different tubular or vesicular  
85 transport carriers, which cannot be identified by light microscopy but only by electron  
86 microscopy. The advent of Correlative Light and Electron Microscopy (CLEM) has  
87 been a welcome development for the field (van der Beek et al., 2022) but the  
88 technology lacks the dynamic aspect making it incapable of tracking protein  
89 movement across various compartments. Moreover, these compartments are  
90 themselves often highly dynamic with a limited lifetime. The unambiguous  
91 identification of endolysosomal compartments by light microscopy is hampered by  
92 the fact that early endosomes mature into late endosomes, during which numerous  
93 changes are expected to occur. Most studies have only focused on Rab5 (early) and  
94 Rab7 (late) endosomal markers, both of which have clear limitations in tracking  
95 endosomal maturation. For example, Rab5 marks endocytic vesicles but also a  
96 variety of early endosomes. In addition, Rab5 plays a role in ER dynamics and  
97 nuclear envelope disassembly (Audhya et al., 2007) and is recruited to kinetochores  
98 (Serio et al., 2011). In the case of Rab7, its localization is not solely restricted to late  
99 endosomes; it can also be found on endolysosomes, lysosomes and  
100 autophagosomes (Borchers et al., 2021; Guerra and Bucci, 2016). Furthermore,  
101 EEA1, which is a commonly used marker for early endosomes, marks only a subset  
102 of early endosomes (Wilson et al., 2000). Finally, the sorting nexins such as SNX1  
103 bind to the highly curved tubular membranes found on early and late endosomes but  
104 also on TENs (Carlton et al., 2004; Shortill et al., 2022). A related issue requiring  
105 close attention is the strict nomenclature of early and late endosomes as identified  
106 by Rab5 and Rab7. Rab5-to-Rab7 conversion takes about two minutes  
107 (Podinovskaia et al., 2021; Poteryaev et al., 2010) yet sorting, recycling and  
108 acidification often takes much longer to occur. The coordination of these events with  
109 Rab conversion is still far from being understood. Nevertheless, it appears clear that  
110 these processes are neither fully completed before Rab5-to-Rab7 conversion nor  
111 only start after the conversion event.

112 Another level of complication emerges when studying the recycling of proteins to the  
113 plasma membrane or the Golgi apparatus. Firstly, there are a multitude of different  
114 pathways as illustrated by the large number of different Rab GTPases, cargo  
115 adaptors and recycling complexes that act in these pathways. Do these different  
116 transport containers emerge from the same endosome as it matures from early-to-  
117 late? Are there different recycling compartments? And if so, how does the cargo  
118 enter these different compartments? Moreover, as different cell types vary in their

119 exo- and endocytic capacity, which is also dependent on the metabolic state and the  
120 stress level perceived by the cells, it is unsurprisingly difficult to come to a unified  
121 one-size-fits-all picture of endosomal recycling. In agreement with many researchers  
122 in the endosomal recycling field, the cargos do not adhere to a single pathway; if  
123 their preferred pathway is blocked the cargos may opt to follow a different route,  
124 albeit with lower efficiency. Even though the TEN can be detected by electron and  
125 light microscopy (Franke et al., 2019; Murk et al., 2003; Rahajeng et al., 2010; van  
126 der Beek et al., 2022), most illustrations of the endosomal recycling pathways places  
127 little to no emphasis on the TEN. This is in part due to our rather limited knowledge  
128 beyond the morphological description of TENs.

129 In this review, we address questions about the role of TEN in recycling and how kiss-  
130 and-run of endosomal vesicles with TEN improve the accuracy, fidelity, and  
131 efficiency in cargo sorting and recycling (Solinger et al., 2020; Solinger et al., 2022).

132

### 133 **The role of TEN in sorting and recycling**

134 Tubular Endosomal Networks (TEN) have been observed adjacent to early/sorting  
135 endosomes. They are described as complex and dynamic structures (Franke et al.,  
136 2019; Klumperman and Raposo, 2014; Murk et al., 2003; van der Beek et al.,  
137 2022)(see [Fig.2](#), [movie 1](#)). The TEN and related organelles can be compared to the  
138 Golgi with regards to the complexity of their sorting processes and seem to be a  
139 long-lived compartment (Maxfield and McGraw, 2004). Surprisingly, cargos from the  
140 trans-Golgi network (TGN) are frequently sorted through early endosomal networks  
141 (Mihov et al., 2015). While TENs can often be observed and visualized, the reason  
142 for cells to produce such a complex structure is not completely understood. A  
143 longstanding hypothesis concerns geometry-based sorting where the mere increase  
144 in membrane surface would be sufficient to segregate recycling cargos away from  
145 the globular sorting endosome (SE) without requiring any sorting signals (Maxfield  
146 and McGraw, 2004). In addition, tubular membranes have been shown to selectively  
147 attract specific lipids (Roux et al., 2005) or proteins (Aimon et al., 2014). This would  
148 lead to a “bulk flow” of cargo into the direction of recycling transporter containers. On  
149 the other hand, more and more sorting motifs for specific protein sorting via cargo  
150 adaptors have been identified (Chi et al., 2015; Cullen and Steinberg, 2018; McNally  
151 and Cullen, 2018). A potential sorting mechanism involving self-assembly through  
152 prion-like domains has also been proposed (Ritz et al., 2014). The main protein  
153 sorting step has been described as happening right at the SE: short tubules  
154 emanating from the globular SE for a limited time from which vesicles (or tubules)  
155 could pinch off, and the remaining tubule would retract (Cullen and Steinberg, 2018;  
156 McNally and Cullen, 2018). Indeed, it has been proposed that the elongated tubules  
157 of the TEN serve solely as transport carriers and that no cargo exchange will happen  
158 after they detach from the sorting endosome (Xie et al., 2016).

159 The TEN itself seems to be enriched in sorting nexins that bind to and stabilize  
160 tubular membranes. Some of these sorting nexins (SNX5 and SNX6) are involved  
161 directly in cargo binding and function as cargo adaptors (Simonetti et al., 2019).  
162 Other sorting nexins (e.g., SNX1, SNX9) could potentially provide a structural

163 component of TEN by binding and tubulating membranes (Carlton et al., 2004;  
164 Pylypenko et al., 2007; van Weering et al., 2012). TEN membranes were also shown  
165 to contain clathrin and AP1 domains that could organize cargo into domains and  
166 vesicles (Klumperman and Raposo, 2014; Stoorvogel et al., 1996). Since TEN are  
167 thought to contain more than 90 % of the cargo for recycling (Griffiths et al., 1989;  
168 Marsh et al., 1986) and show fission/fusion dynamics similar to mitochondria, it  
169 seems likely that a large part of the sorting happens in these compartments. We  
170 envision the formation of cargo enriched domains through a process of membrane  
171 dynamic and diffusion that would enable cargo adaptors like AP1 and SNX5/SNX6 to  
172 connect to cargos and also potentially through the self-assembly of cargos (Fig. 2,  
173 movie 2). The latter pathway could be similar to the kin recognition model proposed  
174 for the retention of Golgi enzymes (Nilsson et al., 1993). Potential “exit sites” would  
175 form, where either new transport carriers could form and pinch off or pre-existing  
176 vesicles could dock via a kiss-and-run mechanism to pick up cargo (Solinger et al.,  
177 2020; Solinger et al., 2022). The well-described mechanisms of cargo sorting  
178 through tubule formation and pinching-off probably also operates on TEN and is  
179 indispensable for the biogenesis of new transport carriers (Chi et al., 2015; Cullen  
180 and Steinberg, 2018; McNally and Cullen, 2018). The main reason that these  
181 processes are not easily observed in HeLa cells is the relatively low frequency of  
182 endocytosis in these cells where most of the cargo in SE derives from the TGN  
183 (Podinovskaia et al., 2021). Also, cancer cells -like HeLa cells- have adapted their  
184 endocytic and recycling pathways to allow enhanced growth and cell migration  
185 (Mellman and Yarden, 2013). In polarized, intestinal cells with high endocytic  
186 throughput, extended TEN can be more readily visualized (Solinger et al., 2020). In  
187 this case, the sorting tubules contain the bulk of the membranes from which sorting  
188 would occur (as shown in Fig. 2).

189 Even though markers for TEN such as Appl1 (van der Beek et al., 2022), MICAL-L1  
190 and syndapin-2 (Farmer et al., 2021; Giridharan et al., 2013; Gleason et al., 2016)  
191 have been described, the exact sorting mechanisms through these compartments  
192 are not understood.

193

### 194 **The conundrum of affinity versus specificity in cargo sorting**

195 Cargo adaptors need to have low affinity for their clients because they need to  
196 dissociate from the cargo when the complex reaches its destination without high  
197 energy demand. Changes in pH or ionic strength should be sufficient to drive the  
198 dissociation. Cargo adaptors come in two flavors: the first type has high specificity  
199 towards cargos, such as subunits of adaptor complexes at the trans-Golgi network  
200 and COPI and COPII coats. In these cases, specific sequence motifs are recognized  
201 (Gomez-Navarro and Miller, 2016; Guo et al., 2014; Michelsen et al., 2007;  
202 Sandmann et al., 2003). For KKXX motifs in the ER-Golgi shuttle, relatively strong  
203 binding has been measured conferring high specificity (Table 1)(Ma and Goldberg,  
204 2013). KDEL motifs bind strongly in the Golgi and are thought to be released in a  
205 pH-dependent manner in the ER (Table 1)(Wilson et al., 1993; Wu et al., 2020). The  
206 other class of cargo adaptors bind with low specificity. These cargo adaptor-cargo

207 interactions are particularly prominent in the endosomal system, in which the  
208 ubiquitination stage and other parameters are read out in the decision to degrade or  
209 recycle. Thus, the cargo adaptor-cargo interactions in the SE are characterized by  
210 low affinity and low specificity. The relationship between affinity and specificity has  
211 been noted previously (Eaton et al., 1995). Essentially, high specificity often  
212 correlates with high affinity binding, as seen for antibody-epitope interactions (Landry  
213 et al., 2015), or between stable tubulin dimers (Montecinos-Franjola et al., 2016)  
214 (Table 1). Cargo adaptors have been measured by different methods to have much  
215 lower binding affinities to their respective cargo motifs (Table 1 and references  
216 therein). These basic physical properties of cargo adaptors and their cargo led to the  
217 conundrum of how to sort proteins faithfully without too many costly errors. Wrongly  
218 sorted cargo would have to be retrieved then re-sorted, which could lead to  
219 additional energetic costs, especially for cells with high cargo throughput.  
220 To solve this conundrum, we propose that cargo can be sorted in several steps. The  
221 first step would occur as described before, and lead to biogenesis of transport  
222 carriers (Chi et al., 2015). In addition to this process, there would also be sorting in  
223 several steps with increasing cargo binding affinities of adaptors (Table 1). Initial,  
224 pre-sorting would happen by bulk flow of cargo into the extended membranes of the  
225 TEN. This would be followed by low-affinity sorting inside the TEN, leading to pre-  
226 sorted “exit sites” or domains with similar cargo in the TEN (Fig. 2, movie 2). The  
227 final steps of sorting would happen with kiss-and-run events using transport carriers,  
228 docking to these pre-sorted domains and enriching for specific cargo each time  
229 (Solinger et al., 2020; Solinger et al., 2022).

230

### 231 **How kiss-and-run helps the sorting process**

232 We recently discovered an unconventional tethering factor, FERARI, in the  
233 endosomal system, that combines tethering and fusion activities with membrane  
234 pinching (Table 2)(Solinger et al., 2020). In an effort to understand the implications of  
235 FERARI on cargo sorting through SE, we developed a theoretical framework in  
236 which kiss-and-run events could solve the cargo sorting problems mentioned above.  
237 We propose that TEN functions as a meeting place for endosomal cargos of different  
238 origins (plasma membrane, endosomes, TGN) (Solinger et al., 2022). In the TEN,  
239 cargos could be pre-sorted by a diffusive mixing and de-mixing mechanism  
240 according to low affinity interactions with cargo adaptors or other cargos with self-  
241 assembly domains (Fig. 2, movie 2). FERARI could already participate in this  
242 process through interactions with cargo adaptors to create specific “exit sites” in  
243 which different cargos would congregate and be transported to the same destination.  
244 FERARI also tethers different types of transport carriers (depending on their  
245 associated Rab GTPase). The following kiss-and-run event allows loading (or  
246 unloading) of cargo to enrich for specific cargos inside the vesicle (Solinger et al.,  
247 2022). This serial process of cargo enrichment solves the second conundrum of how  
248 to reach selectivity with the low affinity and low specificity of cargo adaptors. Several  
249 subsequent steps of cargo enrichment -similar to a distillation process- would allow  
250 for better sorting results.

251 The length of the docking (or “kiss”) of a transport carrier with the TEN would be  
252 determined by two factors: first, a catastrophe/rescue cycle of RME-1/EHD1 spiral  
253 formation on the stalk region between the transport carrier and the TEN (Fig. 3), and  
254 second, the availability of cargo in the stalk region, which could oppose or counteract  
255 pinching forces (by RME-1 itself, actin, and microtubule motors) (Fig. 4).  
256 Measurements of the size of RME-1 or EHD1 spirals around tubular membranes  
257 have shown that the space available inside the tubules is limited (Table 3) (Daumke  
258 et al., 2007; Deo et al., 2018; Pant et al., 2009). Cargos will have to move through  
259 the neck region of the docked vesicle in small packages or even in a single file. On  
260 the other hand, it is conceivable that the formation of an RME-1 spiral could be  
261 disturbed by the presence of cargo in the stalk, which would lead to difficulties in the  
262 pinching-off of the vesicle. Since RME-1 spiral formation and stability depends on  
263 ATP binding, the hydrolysis of ATP to ADP would lead to destabilization of the spiral  
264 and a “catastrophic” spiral depolymerization analogous to what has been proposed  
265 for microtubules (Fig. 3). With FERARI localized at the base of the stalk, a starting  
266 RME-1 subunit could serve as a seed and always reinitiate the spiral formation. A  
267 cycle of polymerization and catastrophic depolymerization would repeat until all  
268 cargo is successfully sorted into a particular transport container. We expect this  
269 polymerization/depolymerization process to take only a few seconds and be  
270 relatively regular, as the polymerization process should always happen with similar  
271 kinetics and the length of the spiral would be constrained by the geometry of the  
272 vesicle and its connection to the TEN (Fig. 3). In the analogous process of endocytic  
273 vesicle formation, the RME-1 related dynamin forms similar spirals (including  
274 pinching-off activity) in about 10 seconds (Shnyrova et al., 2013; Taylor et al., 2011).  
275 We believe that this regular mechanism provides an explanation for the regular  
276 residence times found in FERARI kiss-and-run events (Solinger et al., 2020; Solinger  
277 et al., 2022). Residence times are quantal with recurrent intervals of cargo loading,  
278 presumably caused by the underlying “catastrophe and rescue” mechanism. A  
279 similar effect could also be caused by the loading of defined cargo packages that  
280 would take a defined amount of time to move through the limited opening of the  
281 vesicle. It seems unlikely that the amount of cargo would always be very similar.  
282 Moreover, cargo size and topology would be rather variable and hence the restriction  
283 through the stalk geometry should affect cargo movement through the neck to  
284 varying degree. Thus, loading times would be very different, depending on the type  
285 and concentration of cargo, inconsistent with the regular intervals that were  
286 observed. We therefore prefer the “catastrophe and rescue” model.  
287 The final decision of how many cycles of cargo loading would occur before the  
288 transport carrier is released would be at least partially dependent on the local cargo  
289 availability. We postulate several possible mechanisms of determining cargo  
290 availability: first, the cargo could clog the stalk and thereby directly undermine the  
291 stability of the RME-1 spiral. Second, cargo adaptors on the TEN, like SNX5 and  
292 SNX6, could directly or indirectly influence FERARI and pinching-off. Third, cargo  
293 adaptors on the vesicle could directly tether to FERARI and only let go when  
294 sufficient cargo is present (Fig. 4). The pinching-off would be favored by three

295 factors: First, the polymerization of the RME-1 spiral itself. Second, actin  
296 polymerization could provide a pushing force (similar to the endocytic process), and  
297 third, microtubule motors will try to pull the vesicle away (Fig. 4). The balance would  
298 be tipped by the presence of suitable cargo to the “stay” side. While the successful  
299 sorting of all the local cargo would lead to the “go” signal for the transport carrier.  
300 This model predicts direct interactions of cargo adaptors (e.g. AP1) with FERARI.  
301 We consider these interactions highly likely since FERARI contains several scaffold  
302 proteins with protein-protein interaction domains (e.g., ankyrin, Rabenosyn-5 and  
303 SPE-39).

304 The polymerization of branched actin starting from FERARI could be envisioned by  
305 the function of ankyrin (one of the subunits is UNC-44/Ank1). Roles of ankyrin-like  
306 proteins in connecting endosomes to the actin cytoskeleton have been observed  
307 previously. While Ank2 is able to bind through its ZU-5 domain to PI(3)P membranes  
308 (Qu et al., 2016) other ankyrin-like proteins can also directly interact with Arp2/3, a  
309 regulator of actin branching (shown for VARP/ANKRD27)(Koseoglu et al., 2015), or  
310 bind to Retromer and the WASH complex (which also regulates Arp2/3) (as seen for  
311 ANKRD50)(Kvainickas et al., 2017). While these functions have not yet been  
312 demonstrated for Ank1 and FERARI, it seems that ankyrins have a function in  
313 mediating contacts between endosomal membranes and actin.

314

### 315 **Percolation model of cargo sorting at endosomes**

316 The repeated kiss-and-run of transport carriers on TEN would lead to maturation and  
317 progressive enrichment of specific cargos in vesicles but also in the TEN itself (Fig.  
318 5, movie 3). A similar process has been proposed for the maturation of Golgi stacks  
319 through iterative fractionation (Dunn et al., 1989). The use of successive cargo  
320 enrichment by serial contacts with low affinity binding adaptors is essentially the  
321 same in the movement of cargo through successive Golgi stacks to the TGN  
322 (Rothman, 1981). Contacts between Golgi cisternae with tubules to exchange cargo  
323 more efficiently have also been reported (Glick and Nakano, 2009). While the  
324 geometry of the TEN and Golgi look somehow different, it seems likely that similar  
325 sorting processes govern their function since the cell has to deal with similar  
326 problems in both systems.

327

### 328 **Directionality of cargo flow during kiss-and-run**

329 How could an intrinsically non-directional mechanism like kiss-and-run lead to a net  
330 flow of cargo into recycling vesicles and transport to their destination? The  
331 measurements of binding constants of cargo motifs to adaptors show a possible  
332 solution to this question (Table 1). In our hypothesis, recycling cargo flows from  
333 RAB-5 vesicles, where it is not bound to any particular adaptor, into the TEN, where  
334 it is bound with low affinity to SNX5 or SNX6 adaptors, and finally into RAB-11  
335 vesicles, carrying adaptors with higher binding affinity (AP1) (Solinger et al., 2022)  
336 (Fig. 6, movie 4, Table 1). Binding of degradative cargo to ESCRT-0 on RAB-5  
337 vesicles would ensure that these cargos remain in the degradative pathway (Fig. 6).  
338 This model is based on different RAB-5 endosomal compartments: vesicles derived



339 directly from endocytic events and that could undergo homotypic fusion promoted by  
340 CORVET (Peplowska et al., 2007; Solinger and Spang, 2013). These early RAB-5  
341 vesicles already carry ESCRT-0 to sequester the degradative cargo. They would be  
342 active for kiss-and-run using the FERARI machinery and able to unload recycling  
343 cargo into the TEN. The fusion with a larger RAB-5-positive SE would lead to the  
344 deposition of all the remaining cargo into the SE. These later RAB-5 compartments  
345 would then be proficient in sorting tubule formation and biogenesis of transport  
346 carriers (Fig. 6, movie 4). After the sorting of all the cargo is achieved, RAB-5  
347 compartments would be ready for RAB-conversion to RAB-7 (Kinchen and  
348 Ravichandran, 2010; Podinovskaia et al., 2021; Poteryaev et al., 2010).  
349 In principle, the cargo could flow directly from the SE into the TEN through  
350 connecting tubules driven by membrane curvature and the vastly larger membrane  
351 surface of the tubular network compared to the globular SE (Maxfield and McGraw,  
352 2004). At the same time, a central sorting step in this model is the described  
353 tubulation and pinching-off of vesicles from the SE (Chi et al., 2015; Cullen and  
354 Steinberg, 2018; McNally and Cullen, 2018). This process provides a first sorting  
355 step and produces transport carriers that would undergo kiss-and-run on TEN to  
356 further enrich for the cargo. This step will also be the determining factor for the final  
357 destination of the vesicle as well as the category of cargo that needs to be loaded.  
358 The vesicle generated at the SE would be equipped with specific SNAREs, RABs  
359 and cargo adaptors. The machineries for this vesicle biogenesis have been identified  
360 (Chi et al., 2015).  
361 As discussed above, we doubt that a one-step sorting will be sufficient given the  
362 complexity of cargos to be sorted. For this reason, we postulate further sorting steps  
363 after the initial recycling vesicle has been formed (Fig. 6, movie 4). The higher-  
364 affinity binding cargo adaptors on the newly formed recycling vesicles (AP1, SNX17,  
365 SNX27, see Table 1) will be able to capture cargo during the kiss-and-run  
366 interactions. Wrongly packaged cargo could flow back into the TEN (it would be  
367 untethered), thereby providing a possibility to correct earlier sorting mistakes. This  
368 mis-sorted cargo could even be picked up by a RAB-5 vesicle and brought all the  
369 way back to the SE. It would primarily be attracted by the cogent cargo adaptor in  
370 the TEN (or by cargo self-assembly) to an "exit site" and await the next kiss-and-run  
371 by an appropriate vesicle.

372

### 373 **Conclusion**

374 Our model is in agreement with the observed data that after the SE very little to no  
375 sorting happens in transport carriers (Xie et al., 2016). Most of the sorting would  
376 happen inside the TEN and not in the recycling vesicles themselves. The transport  
377 carriers would not interact in a stable manner with the TEN but only through short-  
378 term kiss-and-run. The adjustments and "proof-reading" of vesicle cargo would  
379 maybe go unnoticed in a global analysis but would still be crucial in the avoidance of  
380 sorting mistakes. TEN as a whole would still contain all cargo types that need to be  
381 sorted but local differences in cargo content between pre-sorted sub-domains may  
382 be rather large. More high-resolution imaging (also resolving events in time, not only

383 space) would be needed to fully understand the processes involved. We observed  
384 changes over the time scale of a few seconds (4 sec in HeLa, 7 sec in intestinal *C.*  
385 *elegans* cells for one kiss-and-run event) (Solinger et al., 2022). The type of imaging  
386 required to obtain the necessary resolution for the highly dynamic events is much  
387 faster than the imaging routinely used for trafficking events. Therefore, kiss-and-run  
388 has so far been completely overlooked and not taken into consideration.

389

## 390 **Acknowledgements**

391

392 We wish to thank Sung Ryul Choi for critical reading of the manuscript. This work  
393 was supported by the Swiss National Science Foundation (310030\_197779,  
394 CRSII3\_141956) and the University of Basel.

395

396

## 397 **Figure legends**

398

399 **Figure 1:** The many shapes of endosomes. Schematic representation of the  
400 endosomal system, showing the degradative pathway on the right and the  
401 recycling/secretory pathway on the left. Incoming material from endocytic vesicles  
402 and from the Golgi are transported to early/sorting endosomes and associated TEN  
403 where sorting occurs. From this hub, the sorted substances can flow to the dedicated  
404 plasma membrane domains (e.g. apical, basal-lateral, adherens junctions), the TGN  
405 or the degradative pathway (late endosomes, lysosomes). While degradation is  
406 achieved through the formation of intraluminal vesicles inside the endosomes,  
407 sorting and recycling happens mainly through tubular-vesicular structures. Since  
408 many of these processes occur in parallel, markers for specific machineries will  
409 overlap on some structures and be different on others. Early/sorting endosomes may  
410 contain Rab5, SNX1, Rab11 and other markers, while later, maturing endosomes will  
411 still have Rab5 and SNX1 but also Rab7 (and no Rab11). Cargo will flow through  
412 these structures and be handed from one machinery to the next. Thus, each marker  
413 by itself can appear to have very different morphological shapes depending on the  
414 combination with other markers and its position in the pathway, e.g. Rab5 might  
415 appear as small vesicles directly after endocytosis, as larger sorting endosomes  
416 associated with tubules, or as even bigger multivesicular bodies, before switching to  
417 Rab7.

418

419 **Figure 2:** Cargo sorting inside the TEN. The TEN is a highly dynamic structure  
420 constantly exchanging membranes through fission and fusion. Left: movie stills from  
421 [movie 1](#), showing the dynamic nature of TEN labelled with mCherry-SNX-1 in *C.*  
422 *elegans* intestinal cells. Right: schematic representation of the process of cargo  
423 sorting through tubule movement and diffusion to form cargo “exit sites” with similar  
424 cargo with the same destination. Shown are self-assembling cargos with prion-like  
425 domains, cargos bound to higher affinity binding adaptors (adaptor 1) that will be  
426 transported directly to their respective membranes, and cargos bound to low affinity

427 adaptors (adaptor 2). The low affinity adaptor (e.g., SNX5, SNX6) will stay in the  
428 TEN and function as preliminary sorting stations where FERARI can also bind and  
429 form “exit sites” for kiss-and-run interactions. On these “exit sites” transport carriers  
430 with higher affinity adaptors can dock and pick up cargo released from the low  
431 affinity adaptors. In this step, a gradual enrichment of specific cargos could be  
432 achieved and account for the precise sorting without having to use high affinity  
433 binding interactions. For the animated model, see [movie 2](#).

434

435 **Figure 3:** 7 seconds away, just as long as I stay, I’ll be waiting. Schematic  
436 representation of the “catastrophe and rescue” hypothesis for regulation of residence  
437 times of vesicles docked through FERARI to TEN. Top: established mechanism of  
438 catastrophe and rescue in microtubules as a comparison. GTP-bound tubulin dimers  
439 will assemble into microtubules, which will undergo a depolymerization event upon  
440 GTP hydrolysis but can be rescued by repolymerization of fresh GTP-bound tubulin.  
441 Bottom: The microtubule mechanism applied to RME-1 spiral formation around a  
442 stalk connecting a vesicle to the TEN. FERARI will always supply at least one RME-  
443 1 subunit as a crystallization point for filament formation. The growth of the RME-1  
444 spiral will be constrained by the length of the stalk region. The stalk region will also  
445 be constrained by the size of the vesicle and the physical properties of the TEN  
446 tubules. We expect the stalk to have a rather consistent length, allowing for a  
447 consistent amount of time for each cycle of polymerization/depolymerization.

448

449 **Figure 4:** Should I stay or should I go? Schematic representation showing positive  
450 and negative mechanisms determining residence time of transport carriers on TEN.  
451 In addition to the process shown in [Fig.2](#), there is an additional level of control to  
452 determine the residence times of vesicles during cargo loading/unloading. Since high  
453 amounts of cargo cause more cycles of “catastrophe and rescue”, it seems  
454 reasonable to assume that cargo availability will play a role in making transport  
455 carriers wait until the cargo is properly loaded. We envision 3 possible mechanisms:  
456 first, a direct interference of cargo in the stalk with the stability of the RME-1 spiral.  
457 Second, a possible regulation through SNX5/SNX6 and FERARI to stop pinching-off  
458 while cargo is still bound. Third, a direct binding/interaction of vesicle cargo adaptors  
459 with FERARI that would only release once binding sites are saturated. We also  
460 hypothesize 3 mechanisms that would promote pinching-off: first, the polymerization  
461 of RME-1 into a spiral. Second, a pushing force generated by branched actin near  
462 the stalk, possibly starting with the ankyrin subunit of FERARI. Third, microtubule  
463 motors pulling forces since it has been shown that these motors are transporting  
464 vesicles and the speed of vesicles suggests active transport along microtubule  
465 tracks. The net outcome of staying or going would be determined by these opposing  
466 forces.

467

468 **Figure 5:** Percolation mechanism of cargo sorting at TEN. Schematic representation  
469 of vesicle movement through the TEN. See [movie 3](#) for an animated version to  
470 appreciate the dynamics of the mechanism. RAB-5 vesicles would move inward from

471 the plasma membrane and fuse with the progressively growing transport carriers by  
472 CORVET. These could also unload recycling cargo by performing kiss-and-run on  
473 TEN structures. The fusion with a larger SE would then be final and any remaining  
474 cargo including all the ESCRT-0 bound cargo for degradation would be unloaded. A  
475 fast-recycling option that bypasses the SE would be available for the recycling cargo  
476 unloaded at an earlier stage. Cargo that was falsely sorted could be recovered and  
477 brought back to the SE for re-sorting. Formation of new transport carriers at the SE  
478 would then provide the next step of sorting and generate vesicles carrying cargo  
479 bound to adaptors. These vesicles would become progressively enriched in cargo  
480 with each successive kiss-and-run event. Again, this would provide an opportunity to  
481 unload wrongly-sorted cargo. The net outcome of this mechanism would be  
482 analogous to Golgi cargo sorting with the TEN being contacted by transport vesicles  
483 moving in opposite directions and enriching cargo by selective binding to cargo  
484 adaptors.

485

486 **Figure 6:** Cargo flow through TEN using kiss-and-run by FERARI. Schematic  
487 representation of cargo movement and directionality during RAB-5 and RAB-11 kiss-  
488 and-run events. See also [movie 4](#) for a dynamic representation of the mechanism. A  
489 first step of RAB-5 vesicle docking to TEN would allow the unloading for fast-  
490 recycling cargo (presumably unbound inside RAB-5 vesicles). The presence of  
491 ESCRT-0 adaptors on these transport carriers would preclude the loss of cargo for  
492 degradation. The large membrane surfaces inside the TEN would ensure cargo  
493 diffusion into the network. Cargo adaptors with low binding affinity would then be  
494 retained in the TEN and distributed to appropriate “exit sites” with similar cargo and  
495 possibly FERARI to be recovered later. The RAB-5 vesicle would then travel to the  
496 SE and fuse with the help of CORVET to deliver all remaining cargo. From the SE,  
497 the well-described mechanism of tubulation, cargo sorting by adaptors, followed by  
498 pinching-off would generate RAB-11 recycling vesicles. RAB-11 vesicles kiss-and-  
499 run would provide opportunities to load additional cargo but also to proof-read and  
500 deliver cargo to appropriate “exit sites” thus providing more precise sorting.

501

## 502 **Data availability statement**

503 Data sharing is not applicable to this article as no new data were created.

504

505

## 506 **References**

507

- 508 Aimon, S., A. Callan-Jones, A. Berthaud, M. Pinot, G.E. Toombes, and P. Bassereau. 2014.  
509 Membrane shape modulates transmembrane protein distribution. *Dev Cell*. 28:212-  
510 218.
- 511 Audhya, A., A. Desai, and K. Oegema. 2007. A role for Rab5 in structuring the endoplasmic  
512 reticulum. *J Cell Biol*. 178:43-56.

513 Borchers, A.C., L. Langemeyer, and C. Ungermann. 2021. Who's in control? Principles of Rab  
514 GTPase activation in endolysosomal membrane trafficking and beyond. *J Cell Biol.*  
515 220.

516 Carlton, J., M. Bujny, B.J. Peter, V.M. Oorschot, A. Rutherford, H. Mellor, J. Klumperman,  
517 H.T. McMahon, and P.J. Cullen. 2004. Sorting nexin-1 mediates tubular endosome-  
518 to-TGN transport through coincidence sensing of high- curvature membranes and 3-  
519 phosphoinositides. *Curr Biol.* 14:1791-1800.

520 Chi, R.J., M.S. Harrison, and C.G. Burd. 2015. Biogenesis of endosome-derived transport  
521 carriers. *Cell Mol Life Sci.* 72:3441-3455.

522 Cullen, P.J., and F. Steinberg. 2018. To degrade or not to degrade: mechanisms and  
523 significance of endocytic recycling. *Nat Rev Mol Cell Biol.* 19:679-696.

524 Daumke, O., R. Lundmark, Y. Vallis, S. Martens, P.J. Butler, and H.T. McMahon. 2007.  
525 Architectural and mechanistic insights into an EHD ATPase involved in membrane  
526 remodelling. *Nature.* 449:923-927.

527 Deo, R., M.S. Kushwah, S.C. Kamekar, N.Y. Kadam, S. Dar, K. Babu, A. Srivastava, and T.J.  
528 Pucadyil. 2018. ATP-dependent membrane remodeling links EHD1 functions to  
529 endocytic recycling. *Nat Commun.* 9:5187.

530 Dunn, K.W., T.E. McGraw, and F.R. Maxfield. 1989. Iterative fractionation of recycling  
531 receptors from lysosomally destined ligands in an early sorting endosome. *J Cell Biol.*  
532 109:3303-3314.

533 Eaton, B.E., L. Gold, and D.A. Zichi. 1995. Let's get specific: the relationship between  
534 specificity and affinity. *Chem Biol.* 2:633-638.

535 Farmer, T., S. Xie, N. Naslavsky, J. Stockli, D.E. James, and S. Caplan. 2021. Defining the  
536 protein and lipid constituents of tubular recycling endosomes. *J Biol Chem.*  
537 296:100190.

538 Franke, C., U. Repnik, S. Segeletz, N. Brouilly, Y. Kalaidzidis, J.M. Verbavatz, and M. Zerial.  
539 2019. Correlative single-molecule localization microscopy and electron tomography  
540 reveals endosome nanoscale domains. *Traffic.* 20:601-617.

541 Giridharan, S.S., B. Cai, N. Vitale, N. Naslavsky, and S. Caplan. 2013. Cooperation of MICAL-  
542 L1, syndapin2, and phosphatidic acid in tubular recycling endosome biogenesis. *Mol*  
543 *Biol Cell.* 24:1776-1790, S1771-1715.

544 Gleason, A.M., K.C. Nguyen, D.H. Hall, and B.D. Grant. 2016. Syndapin/SDPN-1 is required  
545 for endocytic recycling and endosomal actin association in the *C. elegans* intestine.  
546 *Mol Biol Cell.*

547 Glick, B.S., and A. Nakano. 2009. Membrane traffic within the Golgi apparatus. *Annu Rev Cell*  
548 *Dev Biol.* 25:113-132.

549 Gomez-Navarro, N., and E. Miller. 2016. Protein sorting at the ER-Golgi interface. *J Cell Biol.*  
550 215:769-778.

551 Griffiths, G., R. Back, and M. Marsh. 1989. A quantitative analysis of the endocytic pathway  
552 in baby hamster kidney cells. *J Cell Biol.* 109:2703-2720.

553 Guerra, F., and C. Bucci. 2016. Multiple Roles of the Small GTPase Rab7. *Cells.* 5.

554 Guo, Y., D.W. Sirkis, and R. Schekman. 2014. Protein sorting at the trans-Golgi network.  
555 *Annu Rev Cell Dev Biol.* 30:169-206.

556 Kinchen, J.M., and K.S. Ravichandran. 2010. Identification of two evolutionarily conserved  
557 genes regulating processing of engulfed apoptotic cells. *Nature.* 464:778-782.

558 Klumperman, J., and G. Raposo. 2014. The complex ultrastructure of the endolysosomal  
559 system. *Cold Spring Harb Perspect Biol.* 6:a016857.

560 Koseoglu, S., C.G. Peters, J.L. Fitch-Tewfik, O. Aisiku, L. Danglot, T. Galli, and R. Flaumenhaft.  
561 2015. VAMP-7 links granule exocytosis to actin reorganization during platelet  
562 activation. *Blood*. 126:651-660.

563 Kvainickas, A., A.J. Orgaz, H. Nagele, B. Diedrich, K.J. Heesom, J. Dengjel, P.J. Cullen, and F.  
564 Steinberg. 2017. Retromer- and WASH-dependent sorting of nutrient transporters  
565 requires a multivalent interaction network with ANKRD50. *J Cell Sci*. 130:382-395.

566 Landry, J.P., Y. Ke, G.L. Yu, and X.D. Zhu. 2015. Measuring affinity constants of 1450  
567 monoclonal antibodies to peptide targets with a microarray-based label-free assay  
568 platform. *J Immunol Methods*. 417:86-96.

569 Ma, W., and J. Goldberg. 2013. Rules for the recognition of dilysine retrieval motifs by  
570 coatomer. *EMBO J*. 32:926-937.

571 Marsh, M., G. Griffiths, G.E. Dean, I. Mellman, and A. Helenius. 1986. Three-dimensional  
572 structure of endosomes in BHK-21 cells. *Proc Natl Acad Sci U S A*. 83:2899-2903.

573 Maxfield, F.R., and T.E. McGraw. 2004. Endocytic recycling. *Nat Rev Mol Cell Biol*. 5:121-132.

574 Mayor, S., and R.E. Pagano. 2007. Pathways of clathrin-independent endocytosis. *Nat Rev*  
575 *Mol Cell Biol*. 8:603-612.

576 McNally, K.E., and P.J. Cullen. 2018. Endosomal Retrieval of Cargo: Retromer Is Not Alone.  
577 *Trends Cell Biol*. 28:807-822.

578 Mellman, I., and Y. Yarden. 2013. Endocytosis and cancer. *Cold Spring Harb Perspect Biol*.  
579 5:a016949.

580 Mettlen, M., P.H. Chen, S. Srinivasan, G. Danuser, and S.L. Schmid. 2018. Regulation of  
581 Clathrin-Mediated Endocytosis. *Annu Rev Biochem*. 87:871-896.

582 Michelsen, K., V. Schmid, J. Metz, K. Heusser, U. Liebel, T. Schwede, A. Spang, and B.  
583 Schwappach. 2007. Novel cargo-binding site in the beta and delta subunits of  
584 coatomer. *J Cell Biol*. 179:209-217.

585 Mihov, D., E. Raja, and M. Spiess. 2015. Chondroitin Sulfate Accelerates Trans-Golgi-to-  
586 Surface Transport of Proteoglycan Amyloid Precursor Protein. *Traffic*. 16:853-870.

587 Montecinos-Franjola, F., P. Schuck, and D.L. Sackett. 2016. Tubulin Dimer Reversible  
588 Dissociation: AFFINITY, KINETICS, AND DEMONSTRATION OF A STABLE MONOMER. *J*  
589 *Biol Chem*. 291:9281-9294.

590 Murk, J.L., G. Posthuma, A.J. Koster, H.J. Geuze, A.J. Verkleij, M.J. Kleijmeer, and B.M.  
591 Humbel. 2003. Influence of aldehyde fixation on the morphology of endosomes and  
592 lysosomes: quantitative analysis and electron tomography. *J Microsc*. 212:81-90.

593 Nilsson, T., P. Slusarewicz, M.H. Hoe, and G. Warren. 1993. Kin recognition. A model for the  
594 retention of Golgi enzymes. *FEBS Lett*. 330:1-4.

595 Pant, S., M. Sharma, K. Patel, S. Caplan, C.M. Carr, and B.D. Grant. 2009. AMPH-  
596 1/Amphiphysin/Bin1 functions with RME-1/Ehd1 in endocytic recycling. *Nat Cell Biol*.  
597 11:1399-1410.

598 Peplowska, K., D.F. Markgraf, C.W. Ostrowicz, G. Bange, and C. Ungermann. 2007. The  
599 CORVET tethering complex interacts with the yeast Rab5 homolog Vps21 and is  
600 involved in endo-lysosomal biogenesis. *Dev Cell*. 12:739-750.

601 Podinovskaia, M., C. Prescianotto-Baschong, D.P. Buser, and A. Spang. 2021. A novel live-cell  
602 imaging assay reveals regulation of endosome maturation. *Elife*. 10.

603 Poteryaev, D., S. Datta, K. Ackema, M. Zerial, and A. Spang. 2010. Identification of the switch  
604 in early-to-late endosome transition. *Cell*. 141:497-508.

605 Pylypenko, O., R. Lundmark, E. Rasmuson, S.R. Carlsson, and A. Rak. 2007. The PX-BAR  
606 membrane-remodeling unit of sorting nexin 9. *EMBO J*. 26:4788-4800.

607 Qu, F., D.N. Lorenzo, S.J. King, R. Brooks, J.E. Bear, and V. Bennett. 2016. Ankyrin-B is a PI3P  
608 effector that promotes polarized alpha5beta1-integrin recycling via recruiting  
609 RabGAP1L to early endosomes. *Elife*. 5.

610 Rahajeng, J., S.S. Giridharan, B. Cai, N. Naslavsky, and S. Caplan. 2010. Important  
611 relationships between Rab and MICAL proteins in endocytic trafficking. *World J Biol*  
612 *Chem*. 1:254-264.

613 Ritz, A.M., M. Trautwein, F. Grassinger, and A. Spang. 2014. The prion-like domain in the  
614 exomer-dependent cargo Pin2 serves as a trans-Golgi retention motif. *Cell Rep*.  
615 7:249-260.

616 Rothman, J.E. 1981. The golgi apparatus: two organelles in tandem. *Science*. 213:1212-1219.

617 Roux, A., D. Cuvelier, P. Nassoy, J. Prost, P. Bassereau, and B. Goud. 2005. Role of curvature  
618 and phase transition in lipid sorting and fission of membrane tubules. *EMBO J*.  
619 24:1537-1545.

620 Sandmann, T., J.M. Herrmann, J. Dengjel, H. Schwarz, and A. Spang. 2003. Suppression of  
621 coatomer mutants by a new protein family with COPI and COPII binding motifs in  
622 *Saccharomyces cerevisiae*. *Mol Biol Cell*. 14:3097-3113.

623 Serio, G., V. Margaria, S. Jensen, A. Oldani, J. Bartek, F. Bussolino, and L. Lanzetti. 2011.  
624 Small GTPase Rab5 participates in chromosome congression and regulates  
625 localization of the centromere-associated protein CENP-F to kinetochores. *Proc Natl*  
626 *Acad Sci U S A*. 108:17337-17342.

627 Shnyrova, A.V., P.V. Bashkirov, S.A. Akimov, T.J. Pucadyil, J. Zimmerberg, S.L. Schmid, and  
628 V.A. Frolov. 2013. Geometric catalysis of membrane fission driven by flexible  
629 dynamin rings. *Science*. 339:1433-1436.

630 Shortill, S.P., M.S. Frier, and E. Conibear. 2022. You can go your own way: SNX-BAR coat  
631 complexes direct traffic at late endosomes. *Curr Opin Cell Biol*. 76:102087.

632 Simonetti, B., B. Paul, K. Chaudhari, S. Weeratunga, F. Steinberg, M. Gorla, K.J. Heesom, G.J.  
633 Bashaw, B.M. Collins, and P.J. Cullen. 2019. Molecular identification of a BAR  
634 domain-containing coat complex for endosomal recycling of transmembrane  
635 proteins. *Nat Cell Biol*. 21:1219-1233.

636 Solinger, J.A., H.O. Rashid, C. Prescianotto-Baschong, and A. Spang. 2020. FERARI is required  
637 for Rab11-dependent endocytic recycling. *Nat Cell Biol*. 22:213-224.

638 Solinger, J.A., H.O. Rashid, and A. Spang. 2022. FERARI and cargo adaptors coordinate cargo  
639 flow through sorting endosomes. *Nat Commun*. 13:4620.

640 Solinger, J.A., and A. Spang. 2013. Tethering complexes in the endocytic pathway: CORVET  
641 and HOPS. *FEBS J*. 280:2743-2757.

642 Spang, A. 2015. The Road not Taken: Less Traveled Roads from the TGN to the Plasma  
643 Membrane. *Membranes (Basel)*. 5:84-98.

644 Stoorvogel, W., V. Oorschot, and H.J. Geuze. 1996. A novel class of clathrin-coated vesicles  
645 budding from endosomes. *J Cell Biol*. 132:21-33.

646 Taylor, M.J., D. Perrais, and C.J. Merrifield. 2011. A high precision survey of the molecular  
647 dynamics of mammalian clathrin-mediated endocytosis. *PLoS Biol*. 9:e1000604.

648 van der Beek, J., C. de Heus, N. Liv, and J. Klumperman. 2022. Quantitative correlative  
649 microscopy reveals the ultrastructural distribution of endogenous endosomal  
650 proteins. *J Cell Biol*. 221.

651 van Weering, J.R., R.B. Sessions, C.J. Traer, D.P. Kloer, V.K. Bhatia, D. Stamou, S.R. Carlsson,  
652 J.H. Hurley, and P.J. Cullen. 2012. Molecular basis for SNX-BAR-mediated assembly of  
653 distinct endosomal sorting tubules. *EMBO J*. 31:4466-4480.

654 Weinberg, J., and D.G. Drubin. 2012. Clathrin-mediated endocytosis in budding yeast. *Trends*  
655 *Cell Biol.* 22:1-13.

656 Wilson, D.W., M.J. Lewis, and H.R. Pelham. 1993. pH-dependent binding of KDEL to its  
657 receptor in vitro. *J Biol Chem.* 268:7465-7468.

658 Wilson, J.M., M. de Hoop, N. Zorzi, B.H. Toh, C.G. Dotti, and R.G. Parton. 2000. EEA1, a  
659 tethering protein of the early sorting endosome, shows a polarized distribution in  
660 hippocampal neurons, epithelial cells, and fibroblasts. *Mol Biol Cell.* 11:2657-2671.

661 Wu, Z., S. Newstead, and P.C. Biggin. 2020. The KDEL trafficking receptor exploits pH to tune  
662 the strength of an unusual short hydrogen bond. *Sci Rep.* 10:16903.

663 Xie, S., K. Bahl, J.B. Reinecke, G.R. Hammond, N. Naslavsky, and S. Caplan. 2016. The  
664 endocytic recycling compartment maintains cargo segregation acquired upon exit  
665 from the sorting endosome. *Mol Biol Cell.* 27:108-126.

666



**Table 1:** Binding affinities of cargo adaptors in the endosomal recycling pathway

Cargo	Adaptor	K <sub>D</sub>	Method	Publication
CI-MPR motif	SNX5	18 μM	1	[51]
CI-MPR motif	SNX6	36 μM		
CI-MPR motif	SNX32	18 μM		
IncE	SNX5	0.5-1 μM		
APP peptide	SNX17	33 μM	1	[52]
APP peptide	SNX17-FERM	23 μM		
P-selectin	SNX17	2.7 μM	1	[53]
APP peptide	SNX17	22 μM		
APP peptide	SNX27	28 μM		[52]
LRFN2 motif	SNX27-PDZ	1.6 μM	1	[54]
LRFN2 motif	SNX27-PDZ*	< 1.0 μM		
Kir3.3 motif	SNX27-PDZ	15 μM	1	[55]
Kir3.3 motif	SNX27-PDZ*	0.84 μM		
MPR46 tail**	AP1 complex	11-15 μM	2	[56]
Furin cytosolic tail	AP1 μ1	100-200 μM	1	[57]
Furin cytosolic tail (phos.)***	AP1 μ1	22 μM		
Furin cytosolic tail (phos.)***	AP1 μ1	35 μM	2	
TGN38 cytosolic domain	AP2 μ2	58 μM	3	[58]
CWRPKETLYRRF selected peptide	AP4 μ4	7 μM	2	[59]
APP sorting signal	AP4 μ4	28 μM	1	[60]
hWbp1-KEKSD	α-COP	2.9 μM	1	[45]
	β'-COP	3.4 μM		
Emp47p-KTKLL	α-COP	16.1 μM		
	β'-COP	22.5 μM		
YTSEKDEL	Golgi-Erd2	0.078-0.2 μM	4	[47]
ubiquitin	Hrs	127 μM	1	[61]
ubiquitin	STAM	485 μM		
α-Tubulin	β-Tubulin	0.8-0.08 μM	5	[50]
Epitope	Antibody	10-200 pM	6	[49]

1: isothermal titration calorimetry with peptides

2: surface plasmon resonance

3: fluorimetry

4: Scatchard analysis

5: global analysis combining sedimentation velocity and fluorescence anisotropy

6: microarray-based label-free assay

\* with recombinant VPS26  
\*\* contains 3 binding sites  
\*\*\* phosphorylated

**Table 2:** Previously described roles of FERARI members

<b>FERARI member</b>	<b>Interactor</b>	<b>Process</b>	<b>Publication</b>
SPE-39/VIPAS39/VPS16B	VPS-33.2/VPS33B	ARC syndrome, CHEVI, platelet biogenesis	[62-65]
VPS-45/VPS45	Rabenosyn-5	early endosome fusion	[66-69]
RABS-5/Rabenosyn-5	VPS18	function with CORVET/HOPS	[70,71]
RME-1/EHD1	MICAL-L1, Syndapin2, cPLA2 $\alpha$	membrane tubule fission	[72-77]
UNC-44/ANK1	Spectrin	plasma membrane organization	[78-82]
RFIP-2/Rab11FIP5/RIP11	Rab11	endocytic protein recycling	[83-86]

**Table 3:** Size constraints inside dynamin, RME-1/EHD helices.

<b>Helix protein</b>	<b>inner diameter</b>	<b>outer diameter</b>	<b>Method</b>	<b>Publication</b>
dynamin open	20 nm	50 nm	1	[90]
dynamin close	7 nm	40 nm		
dynamin super-constricted	3.7 nm	37 nm		
EHD1	20-60 nm	340 nm	3	[89]
EHD2	25-75 nm	50-100 nm	4	[87]
RME-1	95 nm	120 nm	4	[88]
<b>Cargo</b>	<b>size</b>			
hTfR	11 x 11 nm		2	[91]
Ptch1	6 x 11 nm		1	[92]

1: cryo-EM

2: crystal structure

3: fluorescence microscopy

4: electron microscopy

Figure 1

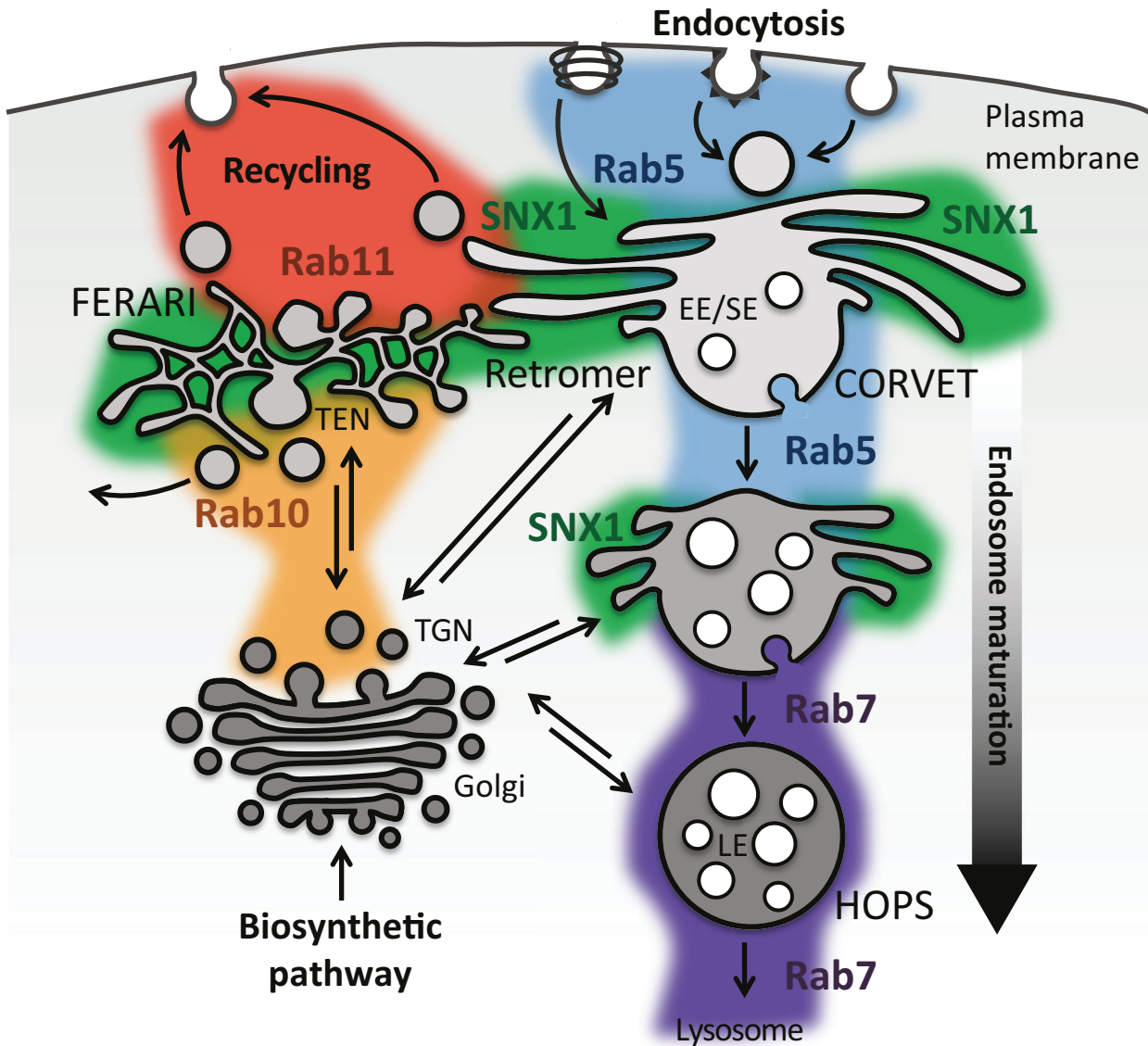
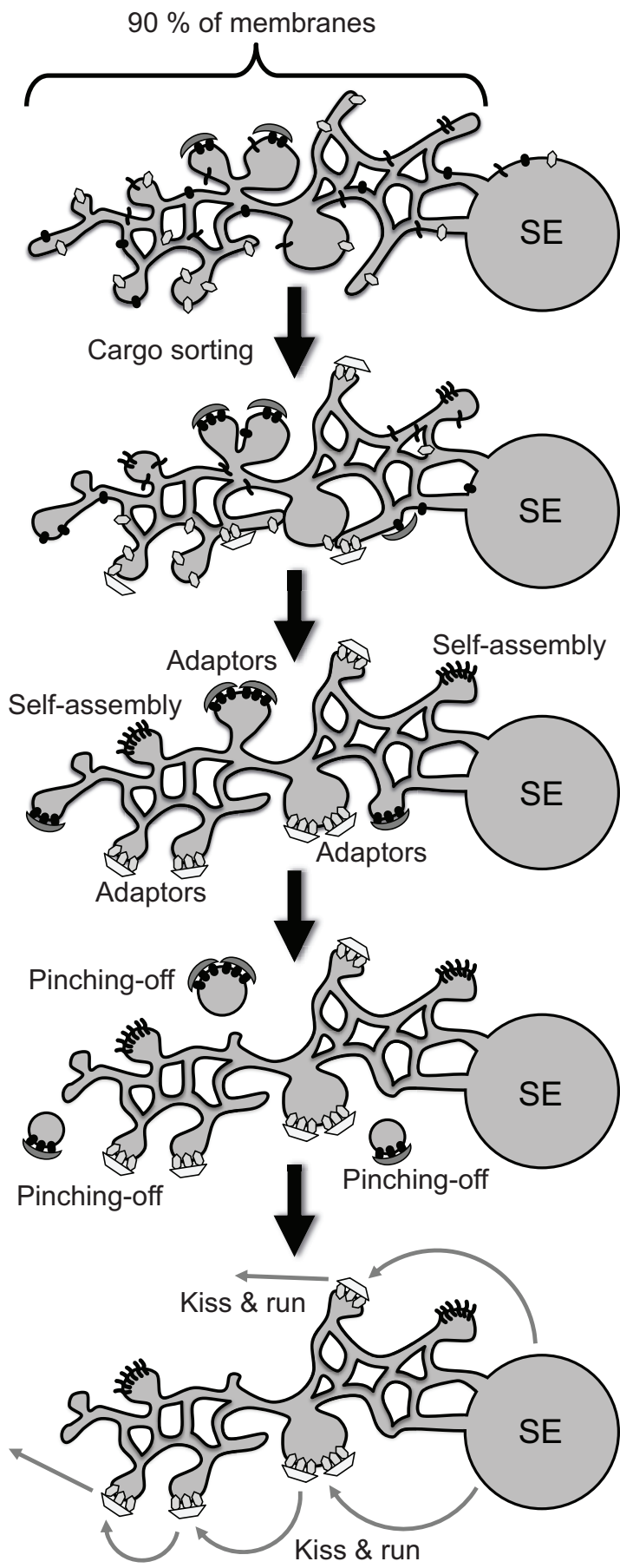
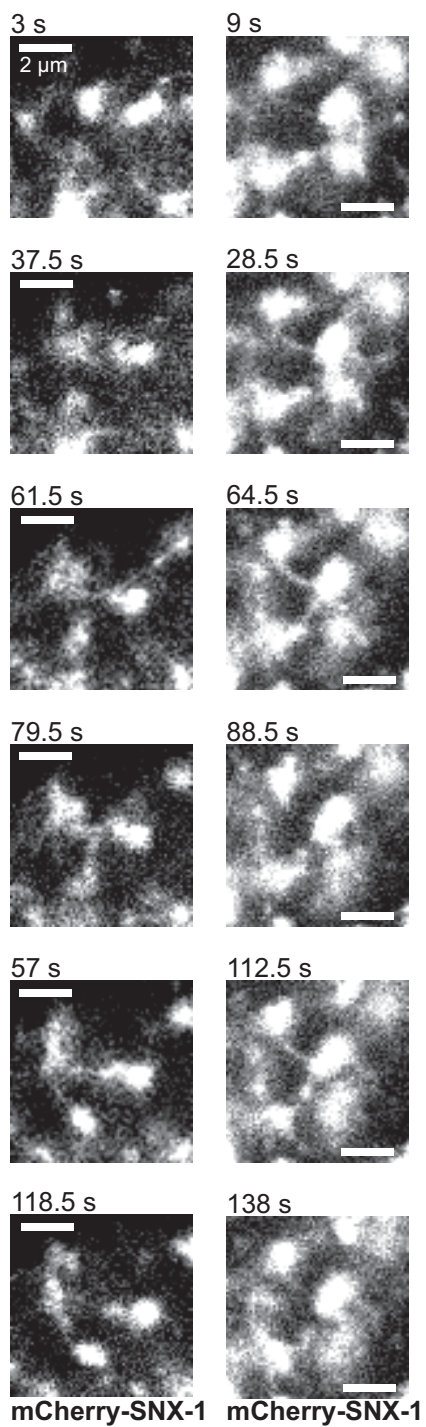


**Figure 2**



- Self-assembling cargo
- Cargo binding adaptor 1
- Cargo adaptor 1
- Cargo binding adaptor 2
- Cargo adaptor 2

Figure 3

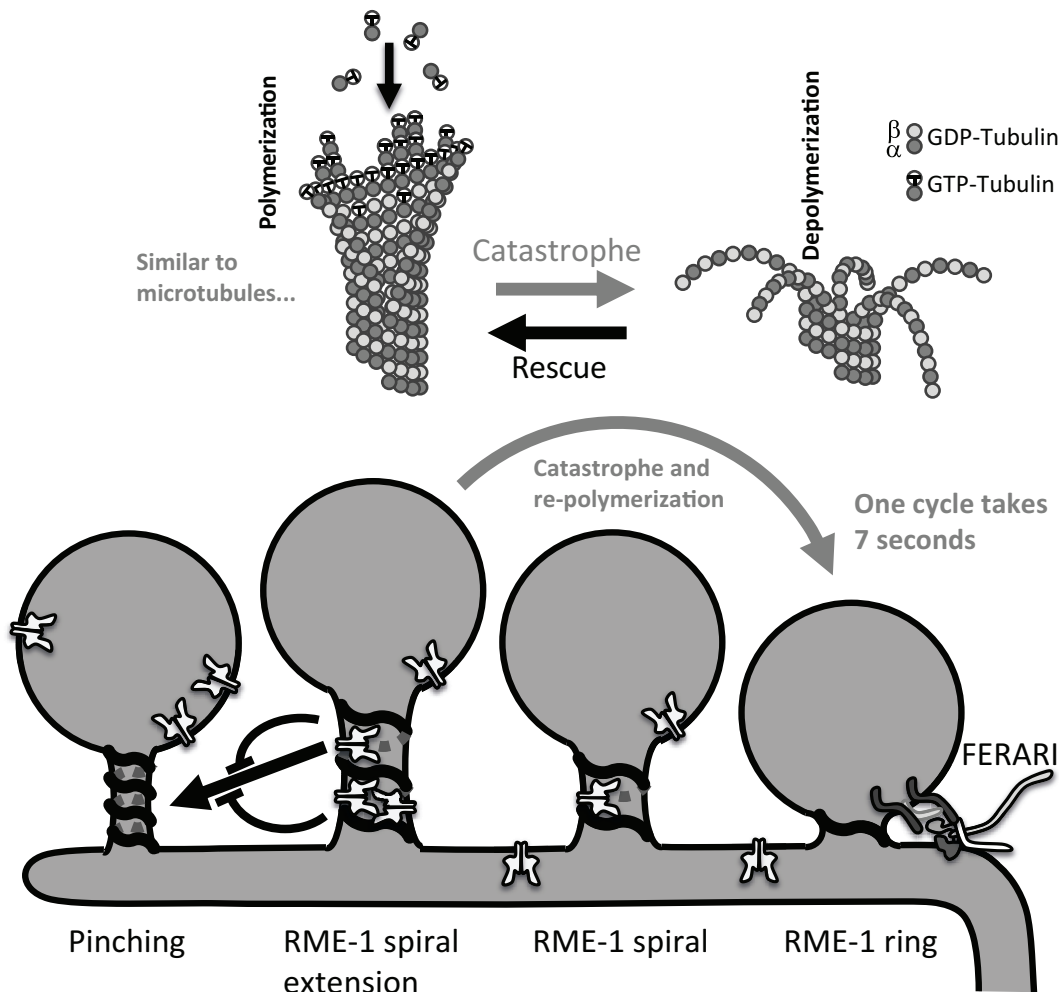


Figure 4

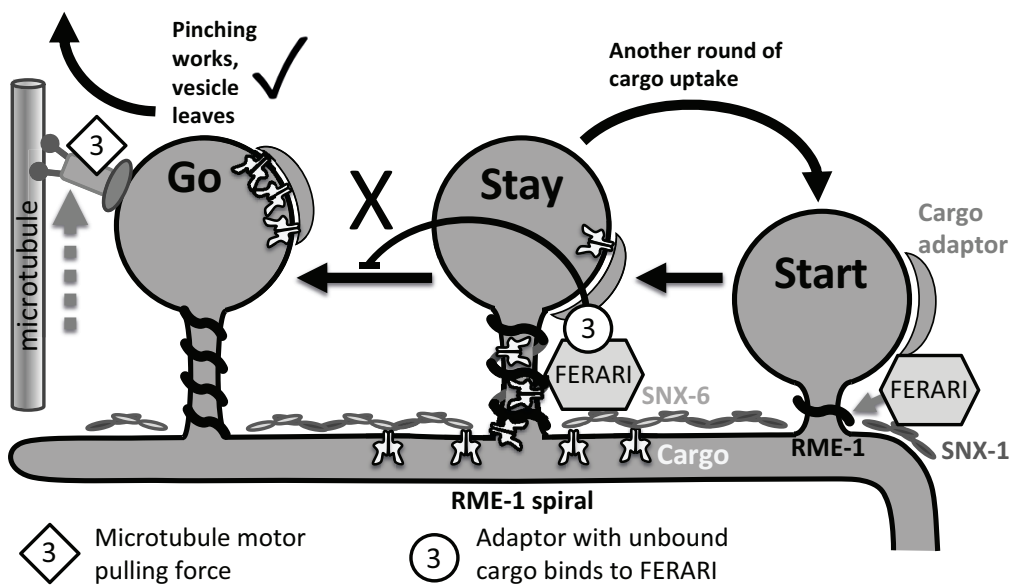
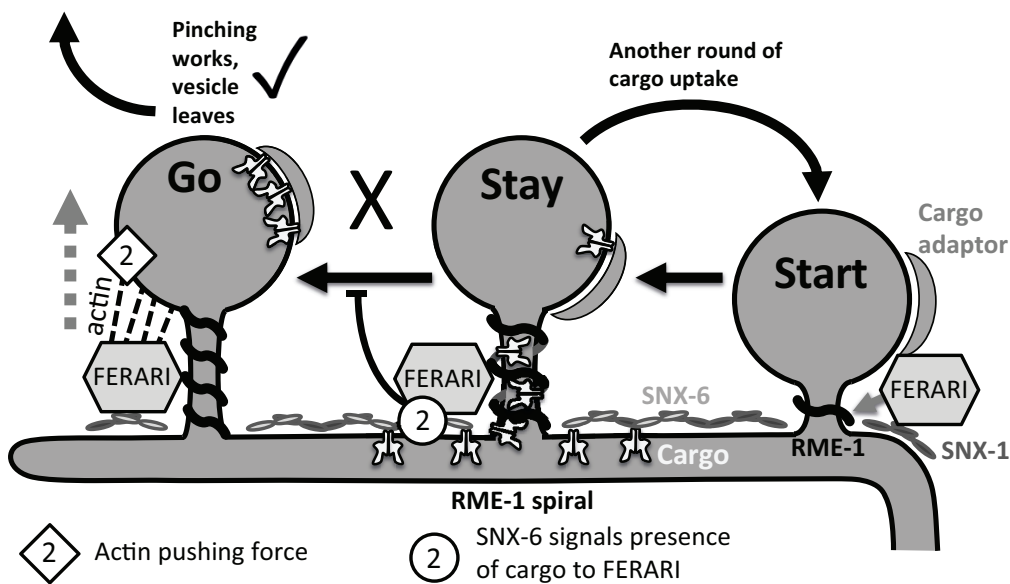
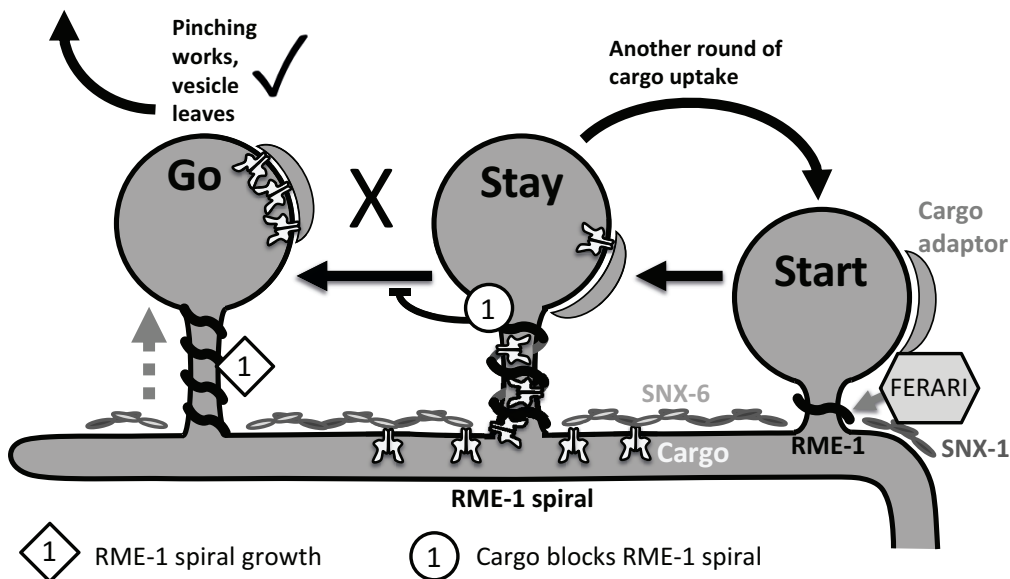




Figure 5

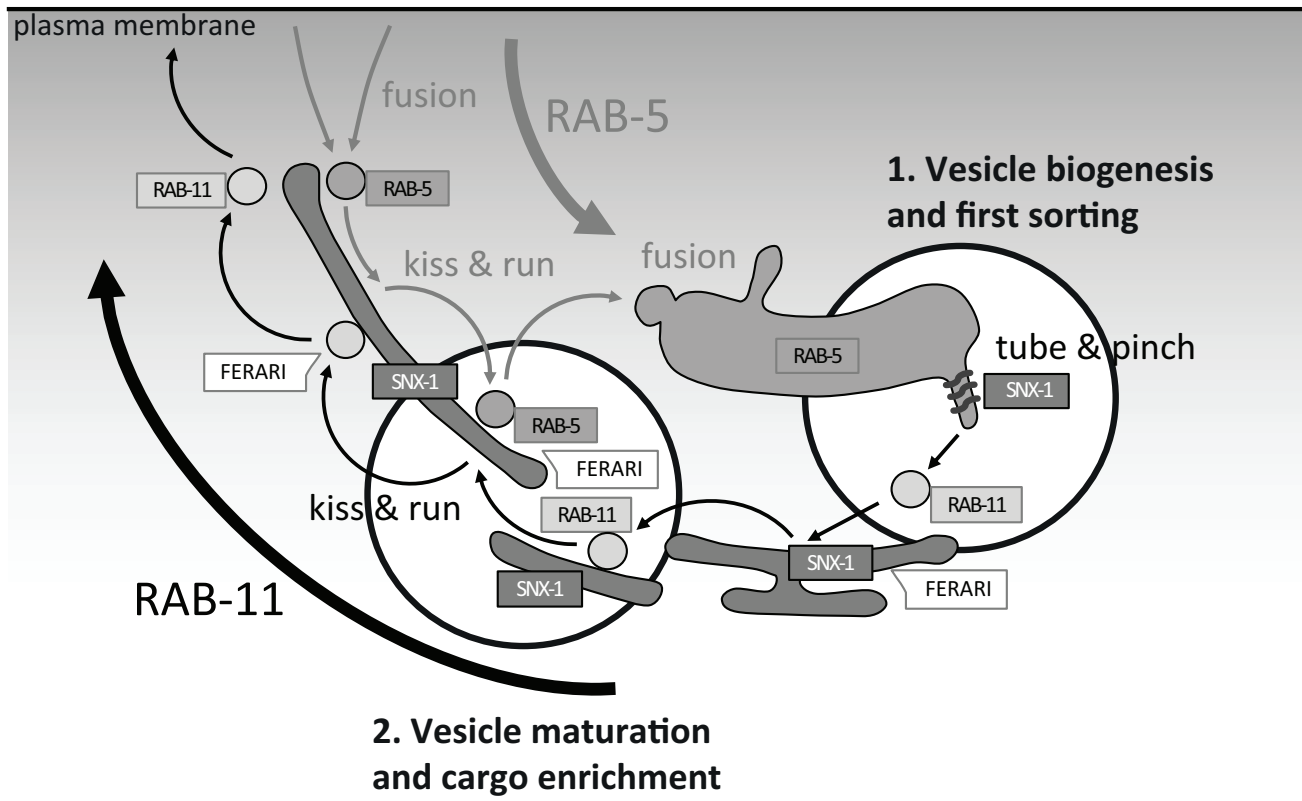


Figure 6

